Fault Segmentation Pattern Controlled by Thickness of Brittle Crust

L. Jiao, Yann Klinger, Luc Scholtes

Fault Segmentation Pattern Controlled by Thickness of Brittle Crust

L. Jiao[1], Y. Klinger[1], and L. Scholtès[2]

[1] Université de Paris, Institut de physique du globe de Paris, CNRS, Paris, France.

[2] Université Clermont Auvergne, CNRS, IRD, OPGC, Laboratoire Magmas et Volcans, Clermont-Ferrand, France.

Corresponding author: Yann Klinger (klinger@ipgp.fr)

Key Points:

- Shear fractures, including earthquake ruptures, are spatially segmented following a pattern inherited from early fracture development
- Numerical simulations show both upward and downward crack propagation when a brittle layer is subjected to strike slip faulting
- Fault segmentation is spatially organized to maintain the material in a stable compressive state of stress through localized tensile ruptures.

This article has been accepted for publication and undergone full peer review but has not been through the copyediting, typesetting, pagination and proofreading process, which may lead to differences between this version and the Version of Record. Please cite this article as doi: 10.1029/2021GL093390.

Abstract

During large earthquakes, seismic sources tend to split in several sub-events that rupture neighboring fault patches called fault segments. The scaling of such segmentation plays a decisive role in earthquake rupture dynamics, especially for strike-slip events. Using numerical modeling we demonstrate that when a pristine layer of brittle material is sheared, the first oblique Riedel fractures nucleate with a regular spacing that is controlled by the thickness of that layer. During later localization of the deformation, those initial fractures control the spatial structuration of the entire fault system. Analyzing the horizontal stress distribution in fault-parallel direction for different ratios between inter-Riedel distance and material thickness, we identify a threshold at 1.5, beyond which the stress switches from compressional to tensional and leads to the nucleation of a new Riedel fracture. Thus, the inter-Riedel segment length appears to be controlled by the vertical distribution of stress along the fault.

Plain Language Summary

Geologic faults, including strike-slip faults, are not continuous smooth structures. Detailed fault mapping and earthquake rupture traces show that they are rather formed by discontinuous segments bounded by jogs and bends. The structure of faults impacts the way a rupture propagates during an earthquake, and eventually where the earthquake rupture starts and stops. Although such spatial organization as long been noted from natural observations and analogue experiments, the physical processes presiding at such organization remain elusive. In this work, we use numerical experiments to show that the fracture pattern is primarily controlled by the thickness of the brittle part of the crust of the Earth and that there is a critical ratio between inter-fracture distance and thickness for which the system is stable and does not need to rupture to accommodate shear. The value, ~1.5, of this ratio is found to be the same in our numerical models, in analogue experiments, and for real earthquake ruptures, pointing to a universal physical process.

1 Introduction

When brittle materials are sheared beyond their elastic threshold, stress is released through fractures (Conner *et al.*, 2003; Taheri *et al.*, 2020). In the case of the crust of the Earth it

may corresponds to earthquake ruptures that produce finite deformation. In the case of continental deformation, when the maximum compressional stress is horizontal, deformation tends to localize along strike-slip faults such as the San Andreas Fault. During medium to large earthquakes with magnitude M≥6.5, most earthquake ruptures involve the entire seismogenic brittle crust, which thickness is 15±5km in continents (Klinger, 2010; Scholz, 1990), and break the ground surface . Field studies (Wechsler *et al.*, 2010), space geodesy (Wei *et al.*, 2011), and seismology (Bilham and Williams, 1985) have long brought evidence that strike-slip earthquake ruptures produce spatially segmented fracture patterns on the ground surface (Fig. 1a), with segment length scaling with the thickness of the brittle crust (Klinger, 2010). These segments are usually bounded by relay zones or bends. Analogue experiments have also hinted at the correlation between the spatial distribution of fractures and the thickness of sheared brittle materials (Cambonie *et al.*, 2019; Lefevre *et al.*, 2020).

Here, we use numerical experiments to test further this correlation, explore the kinematics of fracture growth leading to this peculiar spatial pattern, and derive a universal physical process that explains the relationship between the brittle thickness and the segment length.

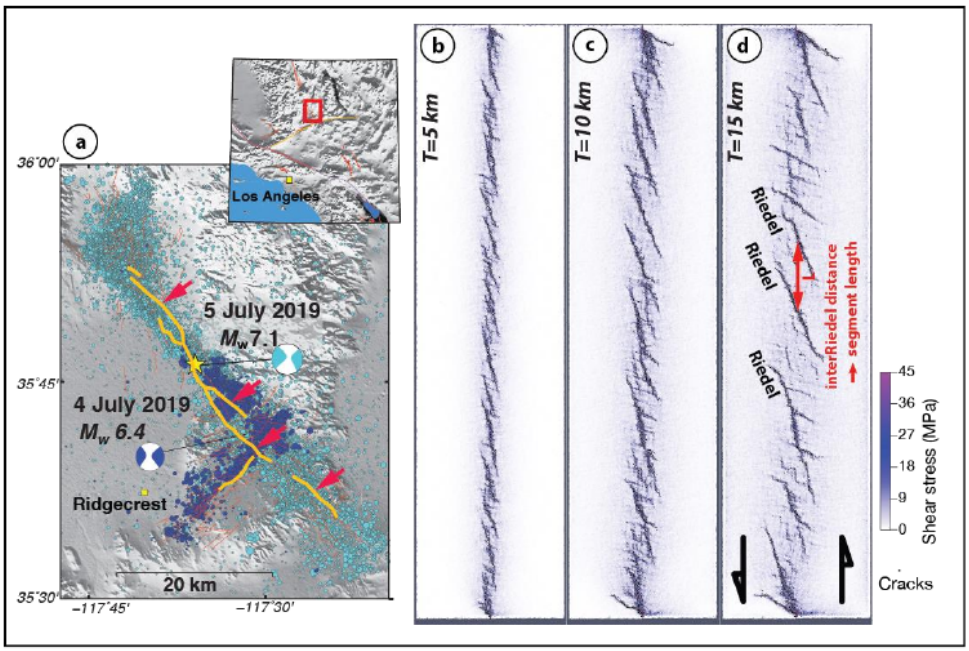

Figure 1: a) Surface rupture for the Ridgecrest Earthquake. Individual segments (Y-shear fractures) are indicated by red arrows (after Ross et al., 2019). b) to d) Top views of left-laterally

sheared DEM models with different thicknesses T. Riedel shears nucleate to accommodate shear. The segment length L corresponds to the inter-Riedel distance L measured along the direction of shear. These segments correspond to Y-shear fractures.

2 Discrete element modeling of fault growth

Geological fault structures, including strike-slip fault systems, have long been studied through numerical modeling (Lynch and Richards, 2001; Segall and Pollard, 1980). However, classical modeling approaches, like the finite element method (FEM) or the finite difference method (FDM), implement faults as pre-existing discontinuities embedded within the numerical medium, therefore hindering mechanical investigation of any spatio-temporal evolution of fault geometry. Conversely, the discrete element method (DEM) enables to simulate the nucleation and propagation of discrete structures by representing the medium as a collection of independent particles interacting one with another through predefined force-displacement laws (Cundall and Strack, 1979; Potyondy and Cundall, 2004; Scholtès and Donzé, 2012). Commonly used to tackle geomechanics problems, the DEM has been successfully applied to study fault system formation or pull-apart basin, including strike-slip settings (Fournier and Morgan, 2012; Liu and Konietzky, 2018; Morgan, 1999; Morgan and Boettcher, 1999).

In this study, we model the continental brittle crust using a bonded particle model implemented in the YADE DEM open-source software (Scholtès and Donzé, 2013; Šmilauer *et al.*, 2015). The particles forming the medium interact through elastic brittle inter-particle laws, which are calibrated so that the emergent bulk behavior of the simulated medium corresponds to the pressure dependent behavior of a typical elastic cohesive brittle rock (see Supplementary Material for details of the methodology, the model formulation as well as for illustration of the emergent behavior). To study strike-slip faulting in the brittle crust, we built up three dimensional models of dimensions equal to *160 km* x *40 km* x *T,* with thicknesses T ranging from 3 km to 30 km (Fig. S2). The models are made up of spherical particles whose radii are uniformly distributed between 170 m and 320 m. The particle density was adjusted as function of the porosity of the particle packing so that the bulk density of the layer corresponds to the crust density (Table S1). Our synthetic crust thus consists of an initially intact and homogeneous elastic brittle layer with boundary conditions set up to mimic a strike-slip tectonic setting. The

top surface of the layer is free, while roller type boundary conditions are defined on the three other sides (the normal displacements along the boundary walls are blocked). In the first stage of the loading sequence, internal stresses are generated by letting the layer stabilize under gravity. Due to the boundary conditions, the maximum compressive stress at the end of this preconditioning stage is vertical and equal to the lithostatic stress, and the horizontal stresses result from the Poisson effect. Then, this pre-stressed layer is sheared horizontally by imposing opposite and parallel constant velocities on each of its half through the lateral and bottom boundaries (Fig. S2). Thus, the only stresses considered in this study relate to the stresses induced by the initial gravitational settling and the subsequent shear loading. Also, the loading rate was chosen to ensure the model response remains quasi-static (rate independent) during the entire deformation process (Fig. S4).

During strike-slip deformation, the localization of deformation is twofold (Naylor *et al.*, 1986). In a first stage, a set of distinct Riedel-shears appears on the top free surface of the medium, which are oblique to the shear direction. During a second stage, Y-shear fractures develop in between successive Riedel-shears, parallel to the shear direction. These Y-shears would eventually coalesce to form a through-going shear fault if the deformation is continued. In our models, the inter-Riedel Y-shears are analogue for fault segments observed in natural strike-slip systems (Fig. 1) and are thus called segments hereafter. To study the influence of the crust thickness on this localization process, we varied the thickness T of our synthetic layer between 3km and 30km (keeping the same model resolution for all cases). For $T \leq 3$ km, no Riedel-shears would appear and a through-going shear fault formed from the beginning of the experiment. Fig. 1b to 1d show examples of surface fault patterns obtained for thicknesses T respectively equal to 5, 10, and 15 km, just before the appearance of the inter-Riedel Y-shears (see additional simulations for other thicknesses in Fig. S6). The associated horizontal offsets are respectively equal to 86 m, 156 m, and 174 m. The average distance between two successive Riedel-shears, distance hereafter called segment length, is determined by dividing the total number of Riedel-shears by the total length of the model (160 km). Our numerical results show that for T=5 km (Fig. 1b), the number of segments is 18, with an average length of 8.9 km per segment, for T=10 km (Fig. 1c), the model produces 11 segments, with an average length of 14.5 km, and for T=15 km (Fig. 1d), the model produces 10 segments, with an average length of 16 km (see Table S2 for Riedel-shears count, segment length, and uncertainties for all simulations). Therefore, our

numerical simulations show that the segment length L increases linearly with the layer thickness T (Fig. 2).

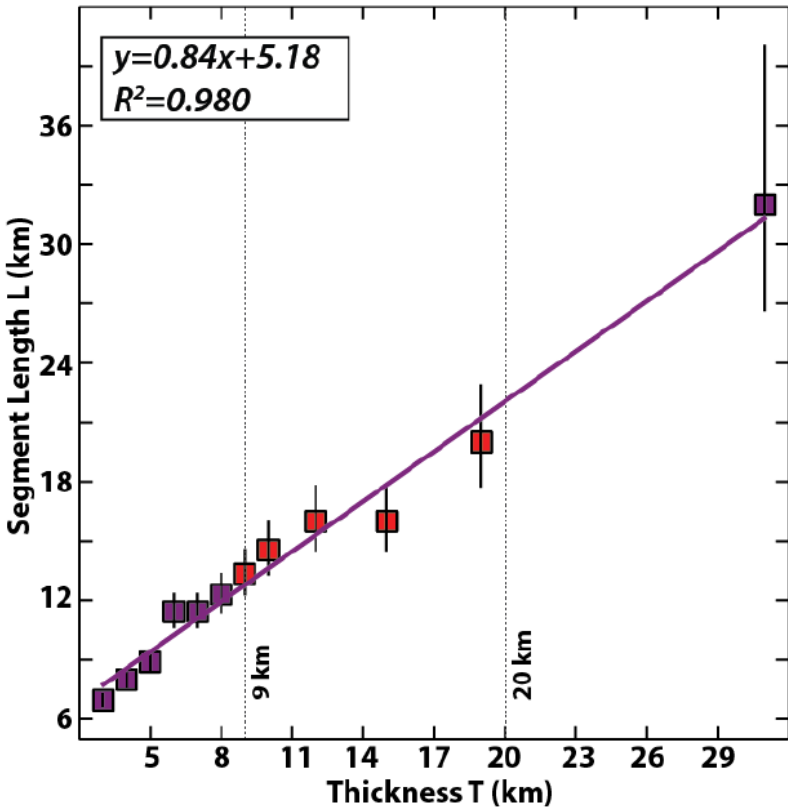

Figure 2: Linear relationship between segment length L and thickness T observed in sheared brittle layers simulated with the DEM. Red squares indicate the range of values commonly accepted for the brittle continental crust thickness (9km≤T≤20km).

3 Temporal evolution of fracture growth

Analogue experiments (Naylor *et al.*, 1986) and theoretical derivation (Mandl, 1999) have suggested that Riedel-shears would initiate at the basal discontinuity of the brittle layer and grow upward, following an helicoidal trajectory, which corresponds to the most effective geometry for energy dissipation (Francfort and Marigo, 1998).

Our numerical simulation reveals that soon after the proto-Riedel shear cracks start to propagate upward from the basal shear zone (step 50 in Fig. 3), some cracks also start to nucleate at the surface (step 65 in Fig. 3). Unlike the cracks that are uniformly distributed along the basal

shear zone, the cracks initiating at the surface are spatially clustered (step 70 in Fig. 3). These cracks then propagate downward (step 80 in Fig. 3) to link with the upward crack front (step 100 in Fig. 3) and to form full-grown Riedel shears (see also animation A1). Eventually, our model shows that the spatial distribution of the crack clusters at the surface of the layer controls the distance between successive Riedel-shears.

The nucleation and propagation of cracks within bonded particle models are driven by the distribution of stress within the simulated medium. Cracks develop in places where inter-particle bonds cannot bear the excess of stress due to either tensile or shear mechanisms. In order to get further insights into the mechanisms at play during the faulting process, we investigated the state of stress on an idealized plane located between two successive Riedel-shears (Fig. 4a) as a function of the ratio between thickness of the model and segment length using a purely elastic 2D model (see Supplementary Material for additional information about model setting).

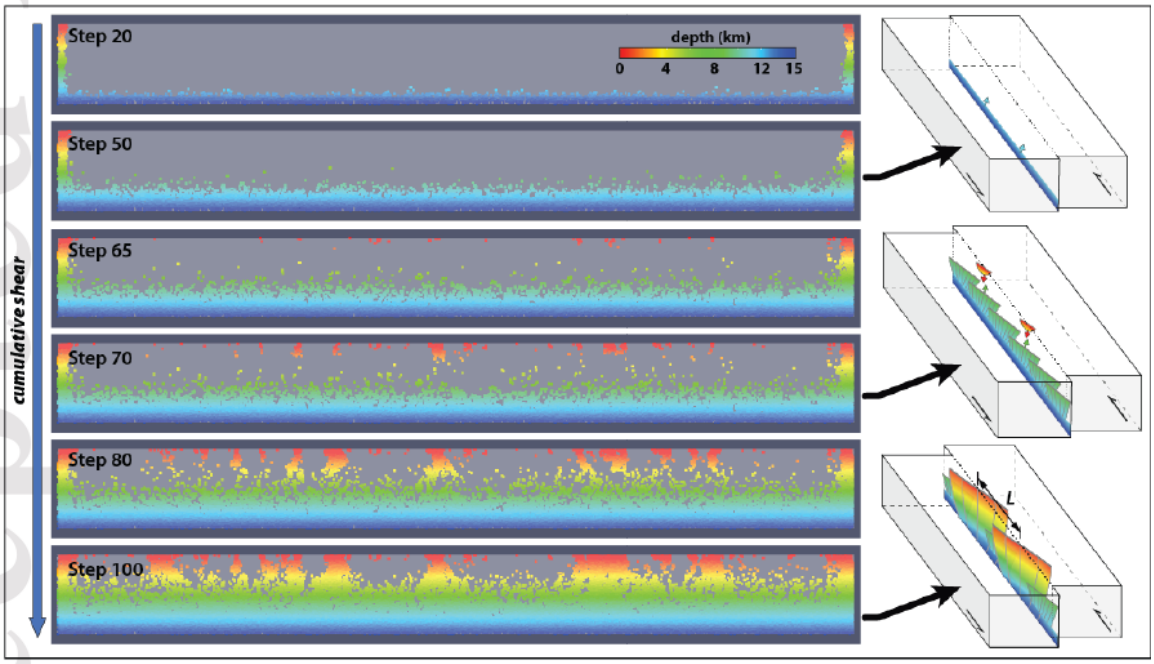

Figure 3: Successive 2km-wide swath cross-sections along the shear direction for increasing shear deformation at the base of the DEM model. Each dot indicates an induced crack colored according to its depth. Step 65 shows nucleation of crack clusters near the layer surface, which later expand downward to form Riedel shears. Sketches to the right illustrate time evolution of cracking within the brittle layer: 1) initiating from the base and propagating upward, 2)

propagation both from top and base of crack fronts, and 3) formation of Riedel shears. L indicates the segment length.

4 State of stress on a plane between two Riedel-shear fractures

Under strike-slip loading conditions the local horizontal stress state at the base of the plane ABA'B' located in-between 2 Riedel-shears (Fig. 4a) is assumed to be primarily of tensile nature (Fig. S7). Building on previous experiments designed to study joint distribution in layered brittle materials (Taixu Bai and Pollard, 2000; T Bai *et al.*, 2000; Yang *et al.*, 2020; Zuza *et al.*, 2017), we set up a 2D elastic model to further investigate the state of stress on the plane ABA'B', as a function of the ratio R between the segment length (AA'), and the layer thickness (AB). The simplified 2D model consists of a layer with a free surface at the top, subjected to pure extensional loading at its base, in order to mimic the deformation process at play in between Riedel-shears (Fig. 4a). Because vertical deformations along AB and A'B' are fixed equal to zero, the extensional loading at the base induces some bending along the vertical axis that in turn generates compression in the ABA'B' plane in the vicinity of the vertical boundaries.

Figures 4b to 4d show the horizontal stress distribution along the vertical strike plane for different values of R=AA'/AB. By convention, compressional stresses are positive. When $R \leq 1.5$, the stress close to the surface is compressional (Fig. 4b and additional examples in Fig. S9). When $R \geq 1.5$, however, the stress at the surface becomes tensional (Fig. 4c and 4d, and Fig. S9). The tensile strength of brittle rocks is significantly lower than their compressive strength, and does not exceed few tens of MPa for crustal rocks (Cai, 2010). Thus, when tensional stress dominates at the surface of the layer, its tensile strength is almost immediately overcome and tension cracks nucleate. These cracks then propagate downward (Fig. 3; also animation A1) to link up with the cracks originating in the vicinity of the basal shear zone, and to form a new Riedel-shear. The creation of this newly-generated Riedel-shear reduces the value of R to a value lower than ~1.5 which, in turn, brings back the stress in a compressional state. The threshold value for R might vary depending on the tensile strength of the materials at play but, nevertheless, this variation stays within a 10% range for rocks (Cai, 2010). A similar process has been found responsible for crack saturation in layered sedimentary rocks and has been characterized by Bai and Pollard (2000). Fig. 4e shows the variation of the horizontal stress at the point M (Table S3), located in the middle of the layer surface, as a function of the ratio R.

When the thickness is significantly larger than the length (ratio R equal to 0.3 or smaller), the stress at point M is close to zero. For R between ~0.3 and ~1.5, compressional stress dominates at point M. As soon as R becomes larger than ~1.5, tensional stresses dominate at point M and the system is unstable, leading to the appearance of a new Riedel-shear and to the subsequent decrease of R to a value close to 1.5. Thus, R~1.5 corresponds to a stable configuration where no additional Riedel would form. Therefore, the thickness of the brittle layer, by controlling the state of stress along the shear plane, exerts direct control over the segment length.

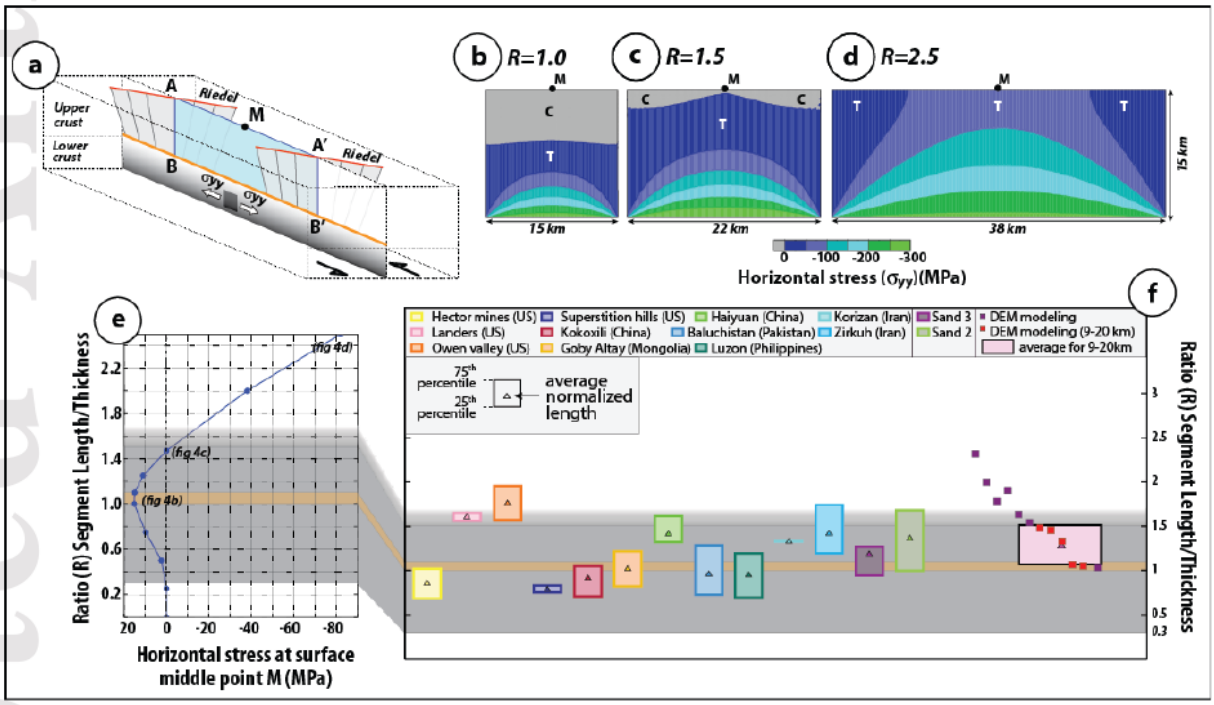

Figure 4: a) Conceptual model where strike-slip imposed at the base induces extension on the plane AA'BB' between two Riedel shears. b) to d) Horizontal stress ditribution (T for tension and C for compression) on the plane AA'BB' as a function of R=L/T, with L the segment length AA' and T the thickness AB=A'B'. Scenario d) is presented only to illustrate stress distribution for R>>1.5, since this configuration is unrealistic as material would already have ruptured. e) Horizontal stress at the surface middle point M as a function of R. The shaded area indicates values of R for which M is in a compressional state of stress. The maximum compressive stress is observed for R~1. Surface tensile cracks are generated for R≥1.5 when the tensile strength of the brittle layer is overcome (between 0 an 10 MPa depending on material). f) Comparison of R values measured in earthquake observations (after Klinger 2010), sandbox experiments (after

Lefevre et al., 2020), and the present study (the pink polygone indicates average for thickness values generally acceped for the continental crust). In each case data are included into the compressional domain.

5 Comparison between field observations, analogue modeling, and numerical results

Figure 4f shows a compilation of data derived from earthquake-rupture field measurements (Klinger, 2010), from analogue fault segmentation experiments (Lefevre *et al.*, 2020), and from our numerical experiments. The values of the ratio R between segment length and thickness of seismogenic crust for continental earthquakes range between 0.3 and 1.6, well within the range predicted by the 2D elastic model. The data derived from DEM models and analogue models are also within the range predicted by the 2D model. Some of the DEM model data, however, fall significantly above the maximum predicted value. This is indeed expected as in both experiments, while one tests a wide range of thickness, one also departs from the mechanical parameter self-consistency that is needed when building a model behaving like the Earth brittle crust. For the models that are in a reasonable range with real brittle crust thickness ($9\ \text{km} \leq T \leq 20\ \text{km}$), however, we find that the data also fall into the same range of values for the ratio R ($1.1 < R < 1.5$). Figure 4f demonstrates that a universal physical process controls the length of fault segments between successive Riedel-shears in different materials subjected to shear, including the crust of the Earth. Fault segmentation in earthquake ruptures is thus directly correlated to the thickness of the crust.

Acknowledgments

Observational datasets used in this study are directly derived from Klinger (2010) and Lefevre et al. (2020).

We thank J. McBeck, an anonymous reviewer, and the editor G. Prieto for insightful comments that helped improve this manuscript. The research was partly supported by the ANR project DISRUPT (ANR-18-CE31-0012). L.J. was funded by SIGMA-2 project.

References

Bai, T., and D. D. Pollard (2000), Fracture spacing in layered rocks: a new explanation based on the stress transition, Journal of Structural Geology, 22(1), 43-57.

Bai, T., D. Pollard, and H. Gao (2000), Explanation for fracture spacing in layered materials, Nature, 403(6771), 753-756.
Bilham, R., and P. Williams (1985), Sawtooth segmentation and deformation processes on the southern San Andreas fault, California, Geophys. Res. Lett., 12, 557-560.
Bischoff, P. H., and S. Perry (1991), Compressive behaviour of concrete at high strain rates, Materials and structures, 24(6), 425-450.
Cai, M. (2010), Practical estimates of tensile strength and Hoek–Brown strength parameter m i of brittle rocks, Rock Mechanics and Rock Engineering, 43(2), 167-184.
Cambonie, T., Y. Klinger, and V. Lazarus (2019), Similarities between mode III crack growth patterns and strike-slip faults, Philosophical Transactions of the Royal Society A, 377, doi: 10.1098/rsta.2017.0392.
Conner, R., W. L. Johnson, N. Paton, and W. Nix (2003), Shear bands and cracking of metallic glass plates in bending, Journal of applied physics, 94(2), 904-911.
Cundall, P. A., and O. D. L. Strack (1979), A discrete numerical model for granular assemblies, Geotechnique, 29(1), 47 - 65.
Duriez, J., L. Scholtès, and F.-V. Donzé (2016), Micromechanics of wing crack propagation for different flaw properties, Engineering Fracture Mechanics, 153, 378-398.
Fournier, T., and J. Morgan (2012), Insights to slip behavior on rough faults using discrete element modeling, Geophysical research letters, 39(12).
Francfort, F., and J. J. Marigo (1998), Revisiting brittle fracture as an energy minimization problem, J. Mech. Phys. Solids, 46(8), 893 -896.
Hart, R., P. A. Cundall, and J. Lemos (1988), Formulation of a three-dimensional distinct element model—Part II. Mechanical calculations for motion and interaction of a system composed of many polyhedral blocks, paper presented at International Journal of Rock Mechanics and Mining Sciences & Geomechanics Abstracts, Elsevier.
Hentz, S., F. V. Donzé, and L. Daudeville (2004), Discrete element modelling of concrete submitted to dynamic loading at high strain rates, Computers & structures, 82(29-30), 2509-2524.
Klinger, Y. (2010), Relation between continental strike-slip earthquake segmentation and thickness of the crust, J. Geophys. Res., 115, doi: doi:10.1029/2009JB006550.
Lefevre, M., P. Souloumiac, N. Cubas, and Y. Klinger (2020), Experimental evidence for crustal control over seismic fault segmentation, Geology.
Liu, Y., and H. Konietzky (2018), Particle- Based Modeling of Transtensional Pull- Apart Basins, Tectonics, 37(12), 4700-4713.
Lynch, J. C., and M. A. Richards (2001), Finite element models of stress orientations in well- developed strike- slip fault zones: Implications for the distribution of lower crustal strain, Journal of Geophysical Research: Solid Earth, 106(B11), 26707-26729.
Maggi, A., J. A. Jackson, D. McKenzie, and K. Priestley (2000), Earthquake focal depths, effective elastic thickness, and the strength of the continental lithosphere, Geology, 28(6), 495 - 498.
Mandl, G. (1999), Faulting in brittle rocks: an introduction to the mechanics of tectonic faults, Springer Science & Business Media.
Morgan, J. K. (1999), Numerical simulations of granular shear zones using the distinct element method: 2. Effects of particle size distribution and interparticle friction on mechanical behavior, Journal of Geophysical Research: Solid Earth, 104(B2), 2721-2732.
Morgan, J. K., and M. S. Boettcher (1999), Numerical simulations of granular shear zones using the distinct element method: 1. Shear zone kinematics and the micromechanics of localization, Journal of Geophysical Research: Solid Earth, 104(B2), 2703-2719.
Naylor, M., G. t. Mandl, and C. Supesteijn (1986), Fault geometries in basement-induced wrench faulting under different initial stress states, Journal of structural geology, 8(7), 737-752.
Potyondy, D. O., and P. Cundall (2004), A bonded-particle model for rock, International journal of rock mechanics and mining sciences, 41(8), 1329-1364.
Scholtès, L., and F.-V. Donzé (2013), A DEM model for soft and hard rocks: role of grain interlocking on strength, Journal of the Mechanics and Physics of Solids, 61(2), 352-369.
Scholz, C. (1990), The Mechanics of Earthquakes and Faulting, 439 pp., Cambridge University Press, New York.
Segall, P., and D. Pollard (1980), Mechanics of discontinuous faults, Journal of Geophysical Research: Solid Earth, 85(B8), 4337-4350.
Šmilauer, V., E. Catalano, B. Chareyre, S. Dorofeenko, J. Duriez, N. Dyck, J. Elias, B. Er, A. Eulitz, and A. Gladky (2015), Yade documentation 2nd ed. the yade project, edited, DOI.

Taheri, M., J. A. Barros, and H. Salehian (2020), Integrated approach for the prediction of crack width and spacing in flexural FRC members with hybrid reinforcement, Engineering Structures, 209, 110208.
Thomas, R. J., and A. D. Sorensen (2017), Review of strain rate effects for UHPC in tension, Construction and Building Materials, 153, 846-856.
Wechsler, N., Y. Ben-Zion, and S. Christofferson (2010), Evolving geometrical heterogeneities of fault trace data, Geoph. J. Int., 182, 551 - 567., doi: doi: 10.1111/j.1365-246X.2010.04645.x.
Wei, S., et al. (2011), Surficial simplicity of the 2010 El Mayor-Cucapah earthquake of Baja California in Mexico, Nature Geoscience, 4, 615-618, doi: 10.1038/NGEO1213.
Yang, H., L. N. Moresi, and M. Quigley (2020), Fault spacing in continental strike-slip shear zones, Earth and Planetary Science Letters, 530, 115906.
Zuza, A. V., A. Yin, J. Lin, and M. Sun (2017), Spacing and strength of active continental strike-slip faults, Earth and Planetary Science Letters, 457, 49-62.